Probes for the early reaction dynamics of heavy-ion collisions at AGS and SPS

A. Dumitru, J. Brachmann, M. Bleicher,
J.A. Maruhn, H. Stöcker, W. Greiner

Institut für Theoretische Physik der J.W.Goethe Universität

Postfach 111932, D-60054 Frankfurt a.M., Germany

Proceedings of the

Workshop on Hydrodynamics at ECT*

Trento (Italy), Mai 12 - 17, 1997

January 16, 2006

Abstract

We discuss the early evolution of ultrarelativistic heavy-ion collisions within a multi-fluid dynamical model. In particular, we show that due to the finite mean-free path of the particles compression shock waves are smeared out considerably as compared to the one-fluid limit. Also, the maximal energy density of the baryons is much lower. We discuss the time scale of kinetic equilibration of the baryons in the central region and its relevance for directed flow. Finally, thermal emission of direct photons from the fluid of produced particles is calculated within the three-fluid model and two other simple expansion models. It is shown that the transverse momentum and rapidity spectra of photons give clue to the cooling law and the early rapidity distribution of the photon source.

1   Introduction

We discuss a three fluid hydrodynamical model for ultrarelativistic heavy-ion collisions in the energy range from BNL-AGS to CERN-SPS. The three fluids are introduced to separate the various rapidity regions observed in high-energy pp-collisions [1]. There it was found that the baryon charge essentially remains close to projectile resp. target rapidity and the energy loss due to particle production is transfered to midrapidity. Assuming that the initial (!) stage of ultrarelativistic heavy-ion reactions is essentially an incoherent superposition of binary NN-collisions leads to a different picture of the early reaction dynamics as compared to one-fluid hydrodynamics. The projectile and target nucleons (as well as the newly produced particles) do not thermalize instantaneously (in the first interaction) but have to undergo several scatterings until kinetic equilibrium is eventually established.

   If the above-mentioned picture of the compressional stage of the heavy-ion reaction is correct, it is natural to introduce three fluids corresponding to the nucleons of the projectile and target (fluids one and two), and to the particles produced around midrapidity (fluid 3). The fluids have to be coupled via local friction forces leading to energy- and momentum exchange. The third fluid is, of course, absent initially and is produced in the course of the collision due to binary collisions between the nucleons of projectile and target. Presently, the rescattering of the produced particles with the nucleons is not taken into account. The interactions between fluids one and two are derived from data on NN-collisions. We employ the parametrization of ref. [2]. A detailed discussion of our model as well as results on baryon stopping, kinetic equilibration, directed and radial baryon flow at AGS were presented in refs. [3]. In contrast to previous multi-fluid models [4], in our model

1. three fluids, corresponding to projectile, target, and produced particles

2. local interactions between the fluids which are based on NN-interactions

3. $(3+1)$-dimensional propagation of all three fluids in space-time

are implemented.

2   Compression shocks

In (ideal) one-fluid hydrodynamics the projectile and target nucleons stop completely (in the center-of-momentum frame) when they touch. Therefore, two shock discontinuities are created [5] that propagate outwards if the velocity of the nucleons is supersonic and if matter is thermodynamically normal, cf. ref. [6] and references therein. Matter between the shock
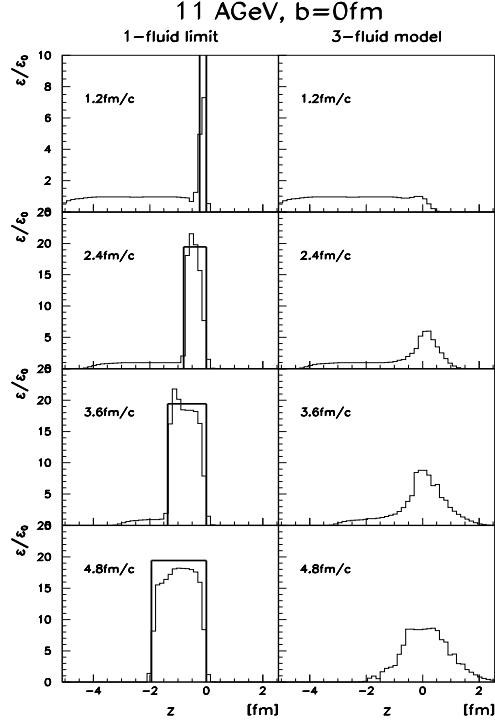
Figure 1: Energy density profile of the projectile fluid along the beam axis (in the center of the reaction, i.e. $x = y = 0$) in one-fluid (left) and three-fluid (right) hydrodynamics as a function of CMS-time.

waves is completely at rest (in the CMS) and reaches the maximal possible energy and baryon density that is compatible with local energy-momentum and baryon number conservation [7, 6]. In fig. 1 we show that the energy density of the shocked projectile matter and the velocity of the shock wave in the three-dimensional calculation agree reasonably well with the values obtained in the semi-analytical one-dimensional shock model (indicated by the box) [7, 6] with our equation-of-state, which treats the baryonic fluids as a non-relativistic ideal gas with compression energy [5]:

$$p(\epsilon, n) = \frac{2}{3}(\epsilon - E_c n) + p_c \quad . \tag{1}$$

For the compression energy, we employ the ansatz

$$E_c = \frac{k_c}{18 n n_0}(n - n_0)^2 + m_N + W_0 \quad , n_0 \approx 0.16 \ fm^{-3} \quad , \tag{2}$$

so that the compressional pressure p_c is

$$p_c = -\frac{dE_c}{dn^{-1}} = n^2 \frac{dE_c}{dn} = \frac{k_c}{18 n_0}(n^2 - n_0^2) \quad . \tag{3}$$

3

However, one also observes that the full-step SHASTA [8] overshoots the correct value for the energy density of the compressed matter at the shockfront. This could probably be cured using a half-step treatment [6], which however requires considerably higher computing times and thus can not be easily implemented in multi-dimensional, multi-fluid models. Once the shock wave has reached the back-side of the projectile nucleus, a rarefaction wave starts to propagate inwards with the velocity of sound, leading to expansion and cooling [9]. This rarefaction wave can be clearly seen in the lower left panel.

In the three-fluid model, the energy density profile looks qualitatively different, cf. right column of fig. 1. One observes that the projectile nucleons cross the symmetry plane $z = 0$, i.e. their mean-free path in the target matter is non-vanishing (in one-fluid hydrodynamics it follows from symmetry arguments that the baryon and energy flow through the plane $z = 0$ vanish). Consequently, no real discontinuity appears, the energy density profile is smooth (within the numerical accuracy). The shock wave (if there is any) is smeared out considerably, which is due to the finite mean-free path (which in turn is linked to the total NN cross section). Also, the smeared-out shock wave obviously leads to less compression and heating of the shocked matter as compared to the discontinuity in the one-fluid limit. The entropy production in the two scenarios remains to be investigated.

3   Kinetic equilibration of projectile and target nucleons

One important issue in ultrarelativistic heavy-ion collisions is whether local thermal equilibrium is established via collisions between the particles. To study this, we have calculated the ratio of the sum of the individual pressures of the projectile and target fluids, $p_1(t, \vec{x}) + p_2(t, \vec{x})$, to the corresponding equilibrium pressure, $p_{eq}(t, \vec{x})$ (and similarly for the baryon densities). This ratio was then averaged over the volume where projectile and target overlap. This ratios approach unity if the relative velocity (at the given space-time point) between the projectile and target fluids becomes comparable to the thermal (resp. Fermi-) velocities of the particles within each fluid (the exact definition is given in ref. [3]). Thus, in one-fluid hydrodynamics it is by definition always equal to one. In contrast, in the three-fluid model (cf. fig. 2) $\langle (p_1 + p_2)/p_{eq} \rangle$ is close to zero in the beginning and reaches unity only after $t_{CM}^{eq} \simeq 2R_{Pb}/\gamma_{CM} = 1.5 \ fm/c$. From this point on local kinetic equilibrium is established and the one-fluid limit is valid for the subsequent expansion. Although this time may look very short, it is significant for observables which are sensitive to the very early reaction dynamics, e.g. directed flow and "hard" thermal photons (or dileptons). Due to the
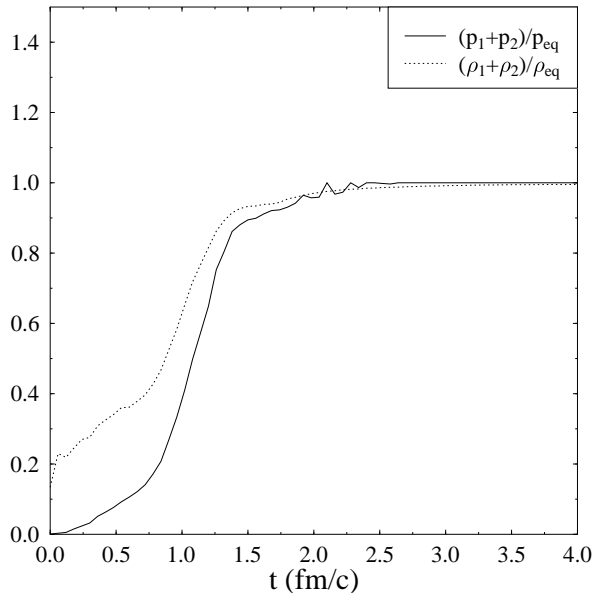
Figure 2: Ratio of the sum of projectile and target pressure (and baryon density) to the equilibrium value as a function of CMS-time; $Pb + Pb$-collisions ($b = 0 \ fm$) at CERN-SPS.

kinetic non-equilibrium in the early stage, the conversion of initial longitudinal momentum into transverse momentum is weaker than in the one-fluid limit.

4 Directed Flow at SPS

We already discussed in ref. [3] that in this model kinetic equilibrium between projectile and target nucleons in the central region occurs on the same time scale as is relevant for the onset of directed nucleon flow. As a consequence, in the three-fluid model the directed nucleon flow is considerably lower and in particular less sensitive to the equation-of-state of the nucleon fluids than in the one-fluid limit. In fig. 3 we show our result for $\langle p_x^{dir}/N \rangle(y)$ for $Pb + Pb$-collisions at CERN-SPS (in calculating this quantity we have neglected thermal smearing of the nucleon momenta; for a definition see ref. [3]). The maximum is on the order of $40 - 50 \ MeV$ and considerably lower than at AGS (due to the fact that the time scale is shorter by roughly a factor of three). Quantitative comparisons to experimental data (directed flow was recently discovered in such reactions [10]) may reveal whether our present model produces enough directed flow or if the contribution of the pressure of the produced particles (as mentioned above, rescattering of produced particles with the projectile and
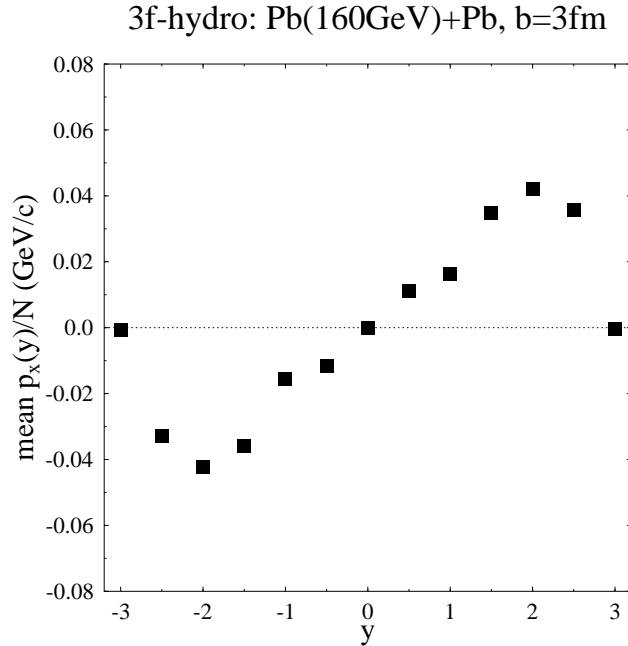
Figure 3: Directed nucleon flow $\langle p_x^{dir}/N \rangle(y)$ in $Pb+Pb$-collisions ($b = 3\ fm$) at CERN-SPS.

target nucleons is presently neglected in our model) is essential. The produced particles are closer in rapidity to the projectile nucleons than the target nucleons (and vice versa), and thus might thermalize faster and exhibit significant pressure on them. Directed nucleon flow at SPS could thus be more sensitive to the equation-of-state of the produced particles than to that of the nucleons themselves. This will be investigated in future work.

5 Thermal photon emission from the third fluid

In our model, in $Pb + Pb$-collisions at CERN-SPS the third fluid locally reaches energy densities up to $\approx 10\ GeV/fm^3$ (for comparison: in the one-fluid limit and for an equation-of-state appropriate for an ultrarelativistic ideal gas, $p = \epsilon/3$, the central region reaches an energy density of $\epsilon/\epsilon_0 = 4\gamma_{CM}^2 - 3$, where $\epsilon_0 \approx 0.15\ GeV/fm^3$ denotes the energy density of nuclear matter in the ground state). We therefore employ an equation-of-state for an ideal QGP (described within the MIT bagmodel) above $T_C = 160\ MeV$. Below T_C, we assume that π, η, ρ and ω are the most abundant particles. The two equations-of-state are matched by Gibbs conditions for phase equilibrium, thus leading to a first-order phase transition.

The temperature of the third fluid in the central cell is depicted in fig. 4. We also compare to two other hydrodynamical models for the expansion of the midrapidity fluid. In scaling
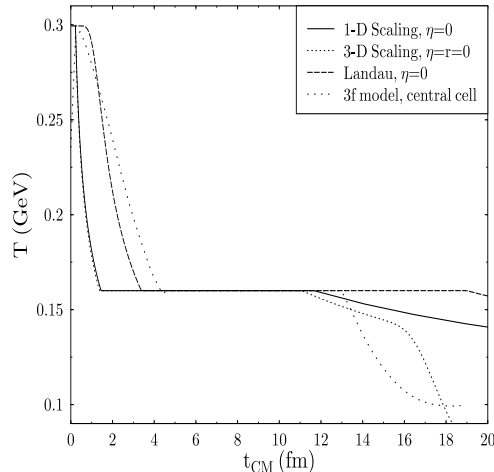
Figure 4: Temperature in the central region as a function of time in various hydrodynamical models, $Pb + Pb$-collisions ($b = 0\ fm$) at CERN-SPS.

hydrodynamics one assumes that the longitudinal flow velocity is $v_z = z/t$ [11] (independent of time), whereas the initial condition for the (one-dimensional) Landau expansion is $v = 0$. In these latter models we assumed an initial temperature of $300\ MeV$ (for the boostinvariant expansion an initial time of $\tau_0 = 0.22\ fm$ was employed). The maximum temperature in the three-fluid model is determined by the coupling terms between fluids one and two (and, of course, by the equations-of-state). The produced particles cool fastest in scaling hydrodynamics, while in the case of a Landau expansion the temperature is constant until the rarefaction waves reach the center. In this latter case one finds the longest-lived mixed phase, due to the fact that we assumed purely one-dimensional (longitudinal) expansion.

The various cooling laws reflect in the transverse momentum distribution of direct photons [12], which can be produced in the QGP- (by annihilation of quarks and antiquarks and Compton-scattering) and hadronic phase (mainly by $\pi - \rho$ scattering) [13]. The faster the cooling of the photon source, the steeper the slope of the photon spectrum. Fitting the spectrum in the region $2\ GeV \leq k_T \leq 3\ GeV$ by an exponential distribution we find "T" $= 260\ MeV$ in the three-fluid model and for the Landau expansion, and "T" $= 210\ MeV$ for the scaling expansion.

The rapidity distribution of thermal photons with transverse momenta much larger than the maximal temperature of the photon source (e.g. $k_T = 2\ GeV$ at SPS) directly reflects the rapidity distribution of the photon source at early times [14], cf. fig. 6. This is due to the fact that "hard" photons do not thermalize, in contrast to e.g. pions. Therefore, in the three-
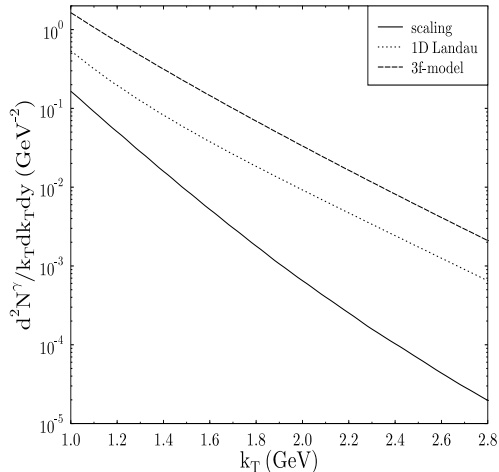
7

Figure 5: Transverse momentum distribution of direct photons at midrapidity ($y^{\gamma}_{CM} = 0$) within various hydrodynamical models, $Pb + Pb$-collisions ($b = 0 \; fm$) at CERN-SPS.

fluid model and in the Landau-expansion case the photon rapidity distribution is strongly peaked around midrapidity and is not proportional to the (squared) rapidity distribution of the pions at freeze-out, as in scaling hydrodynamics.

6 Conclusions

We discussed the compression of projectile and target and showed that the shock discontinuities occuring in the one-fluid limit are smeared out considerably in the three-fluid model. The energy density of the baryons is less than in the one-fluid limit. Most of the energy loss due to stopping goes into production of new particles, leading to the creation of a very hot (temperatures up to 300 MeV at CERN-SPS) third fluid. We compared the cooling of this third fluid in the three-fluid model and two other simple expansion models, longitudinal Landau expansion and longitudinally boostinvariant (plus cylindrically symmetric radial) expansion, and showed how the various cooling laws reflect in the transverse momentum distribution of thermal photons. The rapidity distribution of thermal photons with transverse momenta much larger than the maximal temperature measures the rapidity spread of the photon source at early times (before acceleration leads to broadening). Finally, in the three-fluid model the time scale for kinetic equilibration of the nucleons in the central region is found to be on the order of the Lorentz-contracted nuclear diameter, $2R/\gamma_{CM}$. This leads to a less efficient conversion of initial longitudinal momentum into transverse momentum as
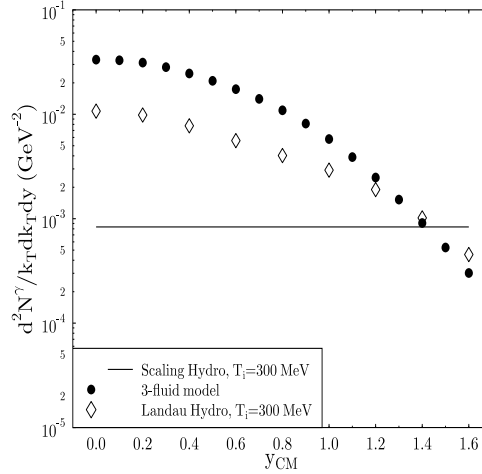
Figure 6: Rapidity distribution of direct photons with $k_T = 2\,GeV$ calculated within various hydrodynamical models, $Pb + Pb$-collisions ($b = 0\,fm$) at CERN-SPS.

compared to the one-fluid limit. As a consequence, the directed flow, which is also created in the early stage of the reaction, is less than in the one-fluid limit.

Acknowledgement

References

[1] V. Blobel et al.: Nucl. Phys. B69 (1974) 454

[2] I.N. Mishustin, V.N. Russkikh, L.M. Satarov: Sov. J. Nucl. Phys. 48 (1988) 454; Nucl. Phys. A494 (1989) 595;
L.M. Satarov: Sov. J. Nucl. Phys. 52 (1990) 264;
I.N. Mishustin, L.M. Satarov, V.N. Russkikh: in "Relativistic Heavy Ion Physics" (eds. D. Strottman and L.P. Csernai), vol. 1, World Scientific (Singapore), 1991, p.179 and Sov. J. Nucl. Phys. 54 (1991) 459

[3] J. Brachmann, A. Dumitru, J.A. Maruhn, H. Stöcker, W. Greiner, D.H. Rischke: preprint UFTP-435/1997 (nucl-th/9703032), Nucl. Phys. A in print;
J. Brachmann, A. Dumitru, M. Bleicher, J.A. Maruhn, H. Stöcker, W. Greiner: Proc. of

the XXXV Int. Winter Meeting Nucl. Phys., Bormio (Italy), 1997 (ed.: I. Iori) (nucl-th 9703044);

A. Dumitru: PhD thesis, Univ. Frankfurt, 1997 (http://www.th.physik.uni-frankfurt.de/~dumitru/lay.ps)

[4] A.A. Amsden, A.S. Goldhaber, F.H. Harlow, J.R. Nix: Phys. Rev. C17 (1978) 2080;
L.P. Csernai et al.: Phys. Rev. C26 (1982) 149;
R.B. Clare, D. Strottman: Phys. Rep. 141 (1986) 177;
H.W. Barz, B. Kämpfer: Phys. Lett. B206 (1988) 399

[5] W. Scheid, R. Ligensa, W. Greiner: Phys. Rev. Lett. 21 (1968) 1479;
W. Scheid, W. Greiner: Z. Phys. 226 (1969) 364;
W. Scheid, H. Müller, W. Greiner: Phys. Rev. Lett. 32 (1974) 741

[6] D.H. Rischke, Y. Pürsün, J.A. Maruhn: Nucl. Phys. A595 (1995) 383; Erratum-ibid. A596 (1996) 717

[7] A.M. Taub: Phys. Rev. 74 (1948) 328

[8] J.P. Boris, D.L. Book: J. Comput. Phys. 11 (1973) 38;
D.L. Book, J.P. Boris, K. Hain: J. Comput. Phys. 18 (1975) 248

[9] D.H. Rischke, S. Bernard, J.A. Maruhn: Nucl. Phys. A595 (1995) 346

[10] H.H. Gutbrod: private communication

[11] K. Kajantie, L. McLerran: Phys. Lett. B119 (1982) 203; Nucl. Phys. B214 (1983) 261;
J.D. Bjorken: Phys. Rev. D27 (1983) 140;
K. Kajantie, R. Raitio, P.V. Ruuskanen: Nucl. Phys. B222 (1983) 152;
H. von Gersdorff, M. Kataja, L. McLerran, P.V. Ruuskanen: Phys. Rev. D34 (1986) 794

[12] D.K. Srivastava, B. Sinha: Phys. Rev. Lett. 73 (1994) 2421;
N. Arbex, U. Ornik, M. Plümer, A. Timmermann, R.M. Weiner: Phys. Lett. B345 (1995) 307;
J.J. Neumann, D. Seibert, G. Fai: Phys. Rev. C51 (1995) 1460;
A. Dumitru, U. Katscher, J.A. Maruhn, H. Stöcker, W. Greiner, D.H. Rischke: Phys. Rev. C51 (1995) 2166;
J. Sollfrank, P. Huovinen, M. Kataja, P.V. Ruuskanen, M. Prakash, R. Venugopalan: Phys. Rev. C55 (1997) 392

[13] J. Kapusta, P. Lichard, D. Seibert: Phys. Rev. D44 (1991) 2774

[14] A. Dumitru, U. Katscher, J.A. Maruhn, H. Stöcker, W. Greiner, D.H. Rischke: Z. Phys. A353 (1995) 187